

# Pilot-Scale Experimental Study on the Coupling of Venturi-Bubbling Reactor to Promote the Absorption of Leaked H<sub>2</sub>S

Guangwen Zhang, Yi Zheng,\* and Yong Zhao Dong

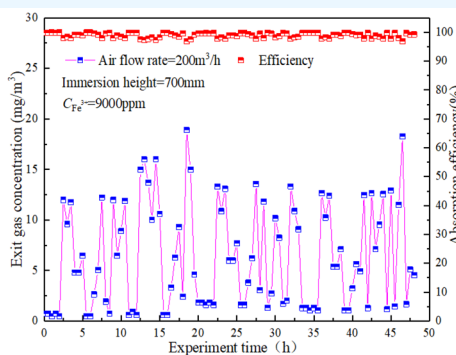
Cite This: *ACS Omega* 2024, 9, 21260–21269

Read Online

ACCESS |

Metrics &amp; More

Article Recommendations



**ABSTRACT:** Natural gas generates varying concentrations of H<sub>2</sub>S during natural formation and extraction, and H<sub>2</sub>S leak accidents are frequent, posing a significant threat to the safety of human life and the environment. Conventional treatment technology equipment is large and does not meet the emergency requirements of the complex topographical gas field. This study aimed to design a pilot-scale method coupling the venturi and bubbling reactors to reduce equipment size and improve emergency capabilities for the absorption of leaked H<sub>2</sub>S. It found that the ring system self-priming venturi reactor, which was suitable only for the coarse treatment of toxic gases, maintained an absorption efficiency of around 50% under most operating conditions, with substantial variations due to changes in process parameters, but that redundancy of the bubbling reactor was high. With the synergistic effect of venturi and bubbling, the coupling process had an extremely high absorption efficiency, basically more than 95%. The experiments also showed that the H<sub>2</sub>S concentration at the outlet of the venturi–bubbling reactor increased with increasing inlet gas concentration and gas volume. The absorption performance improved significantly on increasing Fe<sup>3+</sup> concentration; it increased first and then remained constant, and the optimum Fe<sup>3+</sup> concentration for the absorption of leaked H<sub>2</sub>S was 21 000 mg/m<sup>3</sup>. The absorption performance decreased with increasing submergence height and then remained stable after the size of the inlet approached 600 mm, whereas the overall absorption efficiency of the venturi–bubbling reactor remained constant. The optimum operating temperature range was 10 °C–50 °C. The experimental system kept the outlet concentration below the emergency discharge standard for a continuous period of 48 h following practical use in the gas field and resulting in significant enhancement in mass transfer performance, fully satisfying the emergency requirements.

## 1. INTRODUCTION

H<sub>2</sub>S is a flammable, highly toxic gas with an irritating odor. It is widely produced in industrial processes such as coal and gas extraction, coke ovens, sewage treatment, and petrochemicals.<sup>1–4</sup> When H<sub>2</sub>S gas leaks into the environment, the olfactory threshold is extremely low, with a concentration of 20 ppm already reaching a dangerous value. At a concentration of 700–1000 ppm, the person immediately falls into a coma or dies from respiratory paralysis.<sup>3</sup> Of China's natural gas reserves, those with H<sub>2</sub>S concentrations of more than 1% account for one-fourth of the total reserves. Also, the H<sub>2</sub>S content of some gas fields exceeds 15%, posing an enormous threat to people's lives and property if H<sub>2</sub>S leaks out.

H<sub>2</sub>S removal in the industry is performed using dry<sup>2,5–8</sup> and wet methods.<sup>9–11</sup> Dry methods are dominated by Claus's high-temperature desulfurization and desulfurizer adsorption.<sup>7,8</sup> These processes are relatively mature and could purify sulfur-containing gases well, but the equipment is large and does not satisfy the emergency requirements of H<sub>2</sub>S leakage from gas

Received: February 11, 2024

Revised: April 1, 2024

Accepted: April 22, 2024

Published: May 1, 2024



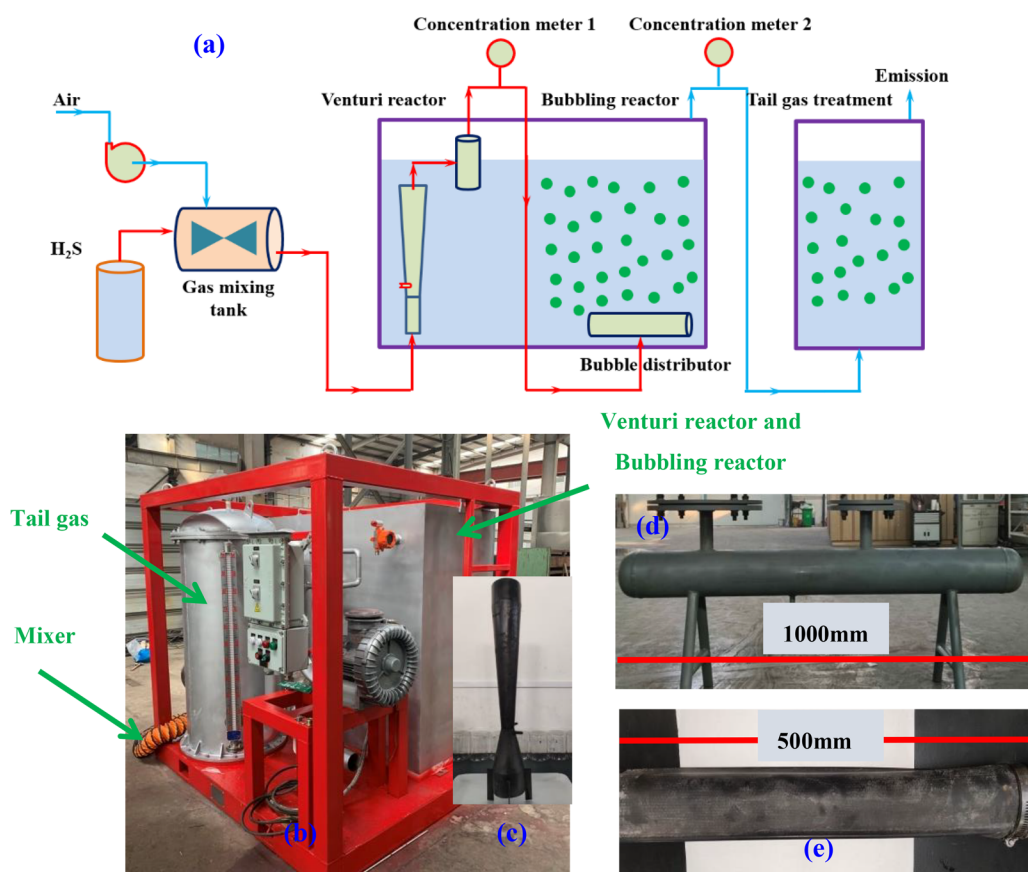


**Figure 1.** Diagram of experimental platform (a) flow diagram (b) experimental device, (c) Venturi reactor, (d) gas distribution tank, and (e) bubbling distributor.

fields with complex terrain. The wet  $\text{H}_2\text{S}$  removal including chemical and physical solvents is a typical gas–liquid two-phase absorption process. The transfer performance is affected by the type of absorbent and the movement characteristics of the gas–liquid interface, and is globally employed to remove sour gas.<sup>9–12</sup>

Extensive research has been conducted to examine the absorption performance of various alkaline solutions, such as sodium hydroxide solution, monoethanolamine, diethanolamine, methyl diethanolamine, 2-amino-2-methyl-1-propanol, and piperazine, in the last decades.<sup>9,13</sup> Üresin et al.<sup>11</sup> investigated the effect of sodium hydroxide solution on the absorptive effect of  $\text{H}_2\text{S}$  and  $\text{CO}_2$  mixture at different residence times in the reactor. They found that the absorptive effect of  $\text{H}_2\text{S}$  increased with increasing residence time, and the maximum absorption efficiency was 80% when the  $\text{H}_2\text{S}$  concentration was above 500 ppm. Yang et al.<sup>14</sup> used numerical simulations to analyze the mass transfer law of  $\text{H}_2\text{S}$  inside the venturi reactor to achieve mass transfer performance using different process parameters. Azizi et al.<sup>15</sup> analyzed the effect of the type of absorbent on the absorption efficiency of a mixture of  $\text{H}_2\text{S}$  and  $\text{CO}_2$ . They pointed out that the presence of  $\text{CO}_2$  significantly inhibited the absorption of  $\text{H}_2\text{S}$  gas. Hence, increasing the selectivity of the absorbent would help reduce the operating costs and improve the absorption performance. Jiao et al.<sup>16</sup> analyzed the effect of centrifugal force on the absorptive effect of  $\text{H}_2\text{S}$  and found that the gas–liquid rotation changed the contact form between the gas phase and the liquid film. Further, the absorption efficiency could reach 99.13%, and the treated  $\text{H}_2\text{S}$  emission concen-

tration was close to the ppb level. The sodium hydroxide solution could effectively absorb the leaked  $\text{H}_2\text{S}$  but could not regenerate it. It is only capable of the emergency filling during actual emergencies because of its reaction with the  $\text{CO}_2$  in the air, thus increasing the difficulty in disposal and the volume of equipment at the accident site.

Therefore, a renewable  $\text{H}_2\text{S}$  wet oxidation process with a long storage time is more valuable for the emergency disposal of  $\text{H}_2\text{S}$  spills.<sup>17–20</sup> For this reason, researchers carried out theoretical and experimental studies on various oxidation systems. Zou et al.<sup>18</sup> synthesized a novel heteropoly acid system that exploited the high selectivity and oxidative properties of heteropoly acids to effectively remove very low concentrations of  $\text{H}_2\text{S}$  with an optimum absorption efficiency of 99.1%. Maia et al.<sup>21</sup> investigated the effect of  $\text{Fe}^{3+}$ -EDTA on the removal of trace amounts of  $\text{H}_2\text{S}$ . The absorption efficiency of  $\text{H}_2\text{S}$  could still reach 99% after 35 min of gas–liquid contact. Vikrant et al.<sup>1</sup> explored the effect of  $\text{Fe}^{3+}$  concentration on the absorption efficiency of  $\text{H}_2\text{S}$ ; the optimum absorption efficiency reached 96% at a  $\text{Fe}^{3+}$  concentration of 200–250 ppm.

At this stage, the main equipment used for the absorption of toxic gases containing  $\text{H}_2\text{S}$  includes bubbling towers,<sup>20,22</sup> venturi scrubbing towers,<sup>14</sup> and packed towers.<sup>23</sup> Still, the conventional equipment is large, cannot be transported over long distances, and is suitable mainly for stable working conditions and not for the emergency requirements of  $\text{H}_2\text{S}$  leaks from gas fields with complex terrain. Meanwhile, scholars have carried out many laboratory-scale performance tests on  $\text{H}_2\text{S}$  tail gas absorption.<sup>1,21,23</sup> However, emergency response

data for pilot-scale H<sub>2</sub>S leaks are still lacking.<sup>9,24</sup> Efficient and intensive processes are urgently required in emergency response. To this end, a pilot-scale method for highly integrative coupling of venturi and bubbling reactors has been developed. Also, the effect of the venturi–bubbling reactor on the absorption efficiency of leaked toxic gases has been experimentally tested, and the effects of process parameters such as flow rate, submersion height, and inlet gas concentration on the absorption efficiency of H<sub>2</sub>S have been researched. Further, field experiments have been carried out at a gas field effluent transfer site.

## 2. EXPERIMENTAL PROCESS

A pilot-scale-leaked H<sub>2</sub>S absorption experimental platform with a maximum gas treatment capacity of 520 m<sup>3</sup>/h was built based on previous findings. The process flow diagram is shown in Figure 1a and 1b. The experimental platform contained a gas distribution system, a toxic gas absorption system, and a tail gas disposal system. The gas distribution system included a gas cylinder, a gas-mixing tank, a mass flow meter, and an explosion-proof axial flow fan. The H<sub>2</sub>S gas in the gas cylinder was mixed with air in the gas-mixing tank. Then, it entered the primary venturi absorber and the secondary bubbling reactor for the gas–liquid contact after the flow fan. The toxic gas absorption system consisted of a primary venturi reactor, a secondary bubbling reactor, and a gas–liquid separator. The venturi and bubbling reactors were used in series after gas–liquid separation. After the reaction, the gas entered the tail gas treatment system, which contained a tail gas treatment tower and an online concentration meter, which was the security device for the experiment. In the experiments, the gas distribution was used to simulate the variation in leaked H<sub>2</sub>S concentration; H<sub>2</sub>S concentrations at the outlets of the venturi and bubbling reactors were obtained by gas chromatography (Agilent 7890B).

The physical diagrams of the mixed gas distribution tank, venturi reactor and the bubbling distributor are shown in Figure 1(c–e). The venturi reactor was self-priming consisting of a tapering nozzle and an outer jacket tube, which could be divided into a liquid convergence section, a throat, and a diffusion section (Figure 1c).<sup>14</sup> The bubbling distributor was a cylindrical distribution tube wrapped around the outer surface with a bubbling membrane. The pore diameter range was 100–600 μm, the diameter of the bubbling distributor was 60 mm, the length was 500 mm, and the installation height was 100 mm from the bottom side of the laboratory table (Figure 1e). The total size of the absorption chamber was 2000 mm, with a width of 1100 mm and a length of 1000 mm. The self-priming venturi reactor was adopted and placed vertically inside the absorption chamber at a height of 200 mm from the bottom. The sulfur solvent, oxidizing agent (complexed iron Fe<sup>3+</sup>/Fe<sup>2+</sup>), and chelating agent in the absorption solution mixture were provided by China Shandong Province Yantai Xinrui Environmental Protection Technology Co. The error of the experimental installation is shown in Table 1.

During the actual experiments, the maximum outlet gas concentration was set to the emergency emission standard (ERPG2, 20 mg/m<sup>3</sup>) in the nonmeasurement upper limit experiments to ensure safety, and the experiments were stopped immediately when the concentration exceeded. The H<sub>2</sub>S concentration at the outlets of the venturi and bubbling reactors were recorded at two different concentration

**Table 1. Experimental Error of Apparatus**

instrument	error
flow fan (NK-GF-8700)	±2.5%
gas chromatography (Agilent 7890B)	±0.05 ps
meter ruler	±0.5 mm
trivalent iron content tester (KYORITSU)	0.1 mg/L
pH meter (BPH-7800)	±0.002 pH
thermocouple	±0.5 K

collection ports in real time during the experiments. The absorption efficiency is calculated as follows:

$$\text{efficiency} = \frac{(\text{inlet concentration} - \text{exit concentration})}{\text{inlet concentration}} \times 100\% \quad (1)$$

## 3. RESULTS AND DISCUSSION

The concentration of the leaked H<sub>2</sub>S in the experiment was 100–10 000 mg/m<sup>3</sup>, the inlet gas volume was 0–520 m<sup>3</sup>/h, and the submerged height of the device was 300–900 mm. The absorption solution was a complexed iron solution, in which the concentration of Fe<sup>3+</sup> was 3000–35 000 mg/m<sup>3</sup>, and the temperature of the absorption solution was 0 °C–50 °C.

The H<sub>2</sub>S concentration in an actual spill is uncertain and fluctuates considerably. The absorption performance was experimentally tested at different inlet H<sub>2</sub>S concentrations to closely match the real accident scenario (H<sub>2</sub>S concentration of 0%–15% in a gas field of Sinopec), with the inlet gas concentration range of 0–10 000 mg/m<sup>3</sup> (Figure 2a and 2b).

Figure 2(a) shows that the venturi reactor outlet concentration increased almost linearly and the absorption performance decreased gradually with the increase in inlet gas concentration. The absorption efficiency of the venturi reactor first decreased rapidly with the increase in inlet gas concentration. After the inlet concentration was higher than 2000 mg/m<sup>3</sup>, the absorption efficiency of the venturi reactor did not change and was maintained at about 45%. Therefore, the venturi reactor alone could not achieve the effective absorption of toxic gas. The analysis also found that the absorption efficiency of the venturi reactor was lower than the experimental findings.<sup>25,26</sup> This was because the process adopted the ring suction self-priming design, which had a sizable liquid diversion, to reduce the pressure drop. And, the atomization rate and droplet size were large, leading to a particular gap in performance. However, compared with equipment with a simpler structure and lower pressure, it was perfectly suitable for the coarse treatment in the process.

The absorption effect of H<sub>2</sub>S by a single bubbler reactor was illustrated in Figure 2(b). The outlet concentration of the bubbler reactor continued to increase with an increase in the inlet concentration. However, when the outlet concentration exceeds 2000 mg/L, it surpasses the acceptable limit of 20 mg/L, failing to meet emergency requirements. It can be observed that a single bubbler reactor exhibits high absorption efficiency, typically exceeding 90%. Nevertheless, its maximum applicable concentration is limited to only 2000 mg/L, which deviates from real-world scenarios encountered in high acid gas fields.

The influence of intake H<sub>2</sub>S concentration on the absorption performance of the venturi–bubbling reactor is depicted in Figure 2(c). As the intake H<sub>2</sub>S gas concentration surpassed 9000 mg/m<sup>3</sup>, the outlet H<sub>2</sub>S concentration of the coupled

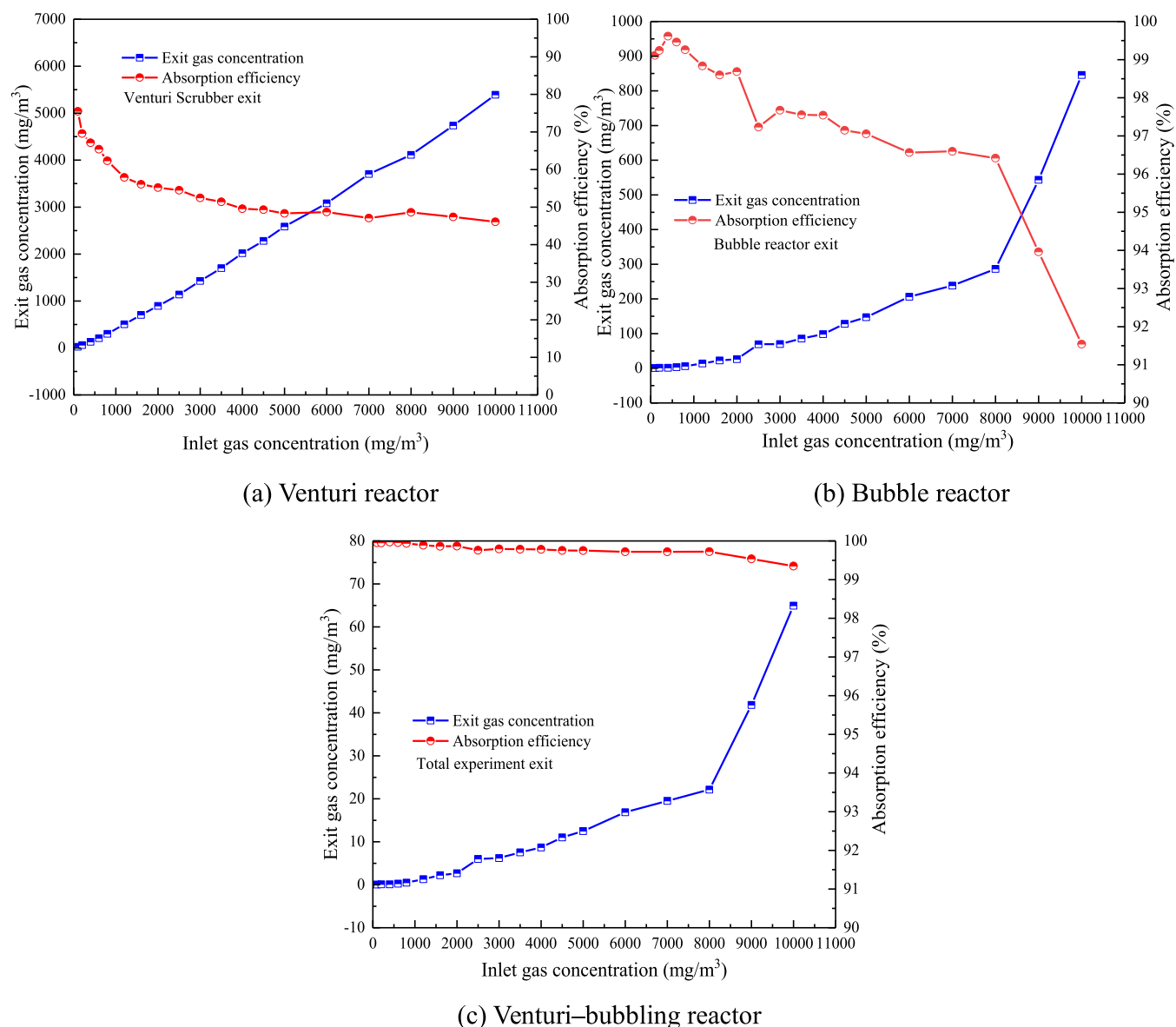


**Figure 2.** Influence of inlet gas on concentration on  $\text{H}_2\text{S}$  absorption performance (gas volume of  $200 \text{ m}^3/\text{h}$ ).

process exceeded  $20 \text{ mg/m}^3$ , exceeding the emergency discharge requirement. At this point, raising the inlet concentration became hazardous as the outlet concentration was already dangerously high. The trials also revealed that the overall absorption efficiency of the linked process for leaked  $\text{H}_2\text{S}$  surpassed 99% and did not fluctuate significantly with the increase in intake concentration. Further investigation revealed that the maximum absorption observed in the bubbling reactor experiments was approximately  $4000 \text{ mg/m}^3$ . This value was significantly lower compared with the individual absorption using the bubbling reactor, which yielded absorption levels of approximately  $6000\text{--}7000 \text{ mg/m}^3$ . This indicated that the effect of gas–liquid separation in the venturi–bubbling reactor reduced the impact on the overall absorption. Experiments showed that the venturi–bubbling reactor had strong absorption performance for leaked  $\text{H}_2\text{S}$  across a wide working range and was flexible.

Figure 3 depicts the influence of the inlet gas flow rate on the absorption performance of leaked  $\text{H}_2\text{S}$ . At the same inlet concentration, the higher the inlet gas flow rate, the higher the

outlet  $\text{H}_2\text{S}$  concentration, but the effect on the absorption performance was not insignificant (Figure 3a). For example, at the corresponding inlet concentration of  $520 \text{ mg/m}^3$ , the venturi–bubbling reactor tail exit concentration increased by a factor of approximately 60 (from  $0.50 \text{ mg/m}^3$  to  $31.28 \text{ mg/m}^3$ ) when the gas flow rate increased from  $50$  to  $500 \text{ m}^3/\text{h}$ . The exit concentration was already higher than the emergency emission standard, but the absorption efficiency of the Venturi–bubbling reactor only decreased from 99.89% to 94.52%.

The analysis found that the absorption efficiency continued to decrease with the increase in gas velocity for the venturi reactor. The lowest absorption efficiency was only 35.62%, a more than 50% decrease from the efficiency under optimum operating conditions. It was because the absorption performance of the venturi reactor was influenced by the amount of absorbent solution induced, atomization rate, and droplet size. The droplet diameter increased and the atomization rate decreased with increasing inlet gas flow rate. Both significantly deteriorated the overall mass transfer in the ring system self-priming venturi reactor used in the experiments. The amount

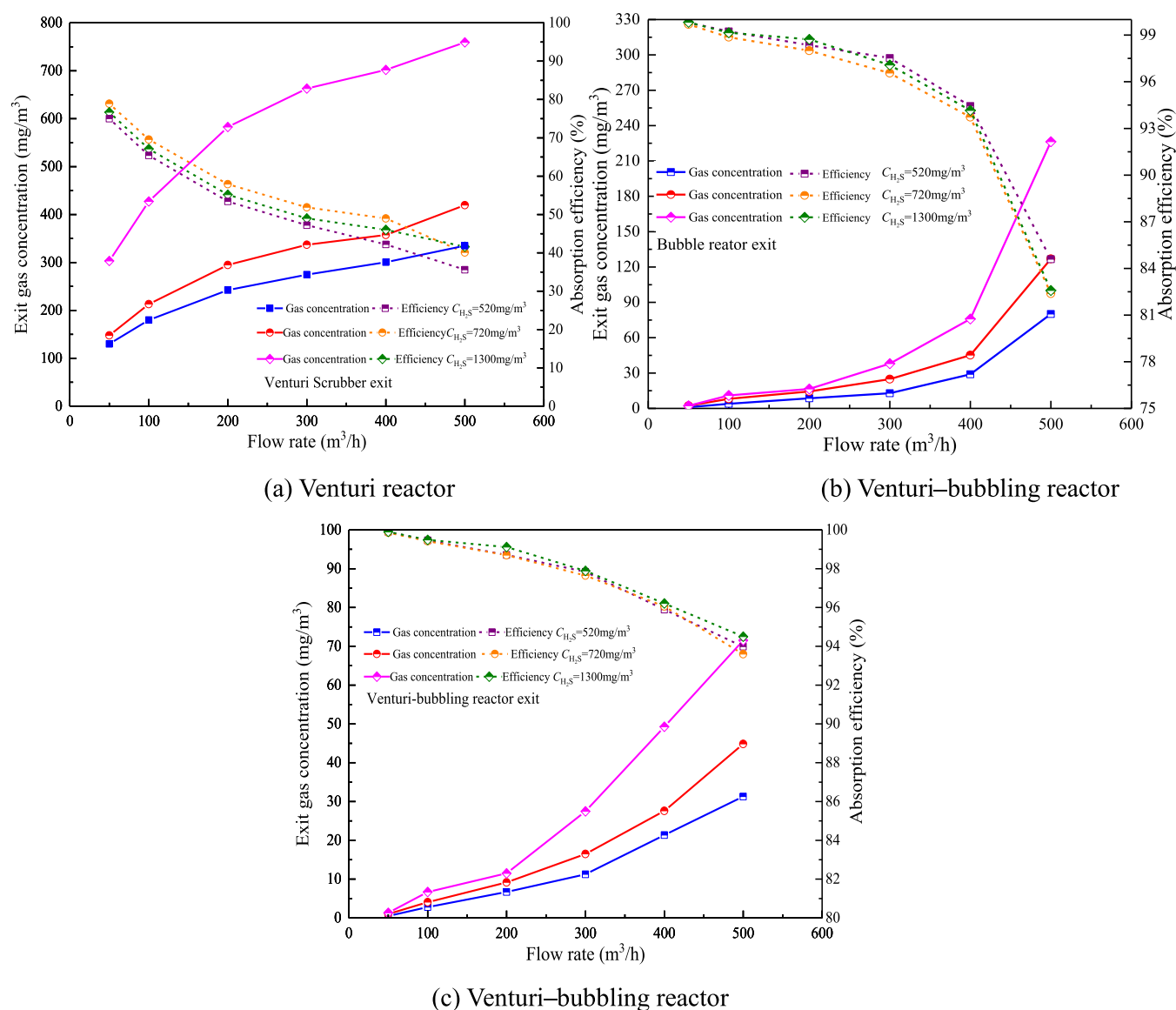


**Figure 3.** Effect of gas flow rate on H<sub>2</sub>S absorption performance.

of absorbent solution induced increased with the increase in inlet gas flow rate; it first increased and then remained constant. Also, the droplet diameter and the atomization rate increased so that the absorption performance of the venturi reactor decreased rapidly with increasing gas volume when the absorbent solution diversion reached a bottleneck.

Further analysis also revealed that, on the one hand, the increase in gas flow rate intensified the liquid tumbling inside the absorption solution, increased the gas–liquid interface, accelerated the diffusion of low-concentration gas-phase components into the liquid-phase components, and promoted gas–liquid contact mass transfer in the bubbling reactor. However, the increase in gas flow rate decreased the residence time of the gas in the absorption solution, which reduced the gas–liquid mass transfer. Therefore, coupling the venturi and bubbling reactors did not significantly reduce the mass transfer performance of the bubbling reactor. However, as the absorption performance of the venturi reactor decreased significantly, the overall performance showed a significant increase in the concentration of the H<sub>2</sub>S gas leaving the reactor with an increasing inlet gas flow rate.

Figure 4 reveals the effect of submersion height on the absorption performance of leaked H<sub>2</sub>S. The submersion height influenced the amount of absorption solution induced by the venturi reactor, atomization rate, and residence time of H<sub>2</sub>S gas. If the submersion height was too low, then the stable operation of the venturi and bubbling reactors was not favored. When the submersion height was too high, the absorption resistance increased. In an environmental emergency, the gas could not pass through the absorption solution bed and a discontinuous upwelling of liquid occurred, deteriorating the mass transfer. The static pressure head of the fan used in the experiment was 30 kPa. Therefore, the submergence height of the bubbling reactor was chosen to be between 300 to 900 mm, and the venturi reactor was installed 200 mm higher than the bubbling reactor, with a submergence height of 100–700 mm. As shown in the graph, the outlet concentration of H<sub>2</sub>S gas decreased with increasing submersion height and subsequently reached a stable level. After the inlet height approached 600 mm, the overall absorption efficiency of the venturi–bubbling reactor remained constant and the absorption efficiency exceeded 97%. At submersion heights below

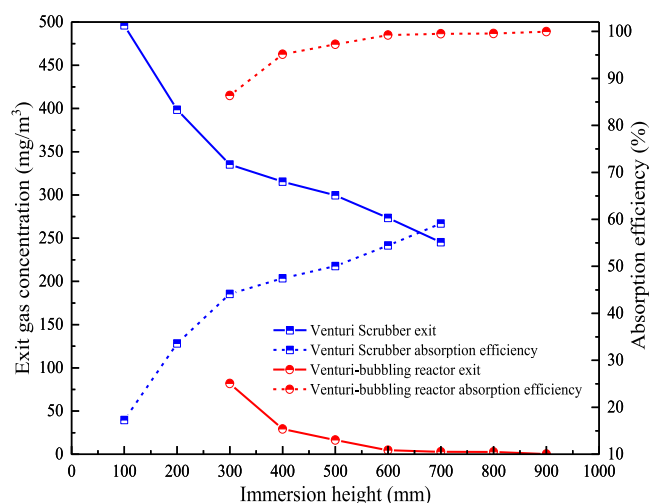


Figure 4. Effect of immersion height on  $\text{H}_2\text{S}$  absorption performance.

400 mm, the outlet gas concentration exceeded the emergency discharge standard. The mass transfer performance deteriorated significantly after that, leading to the need to critically monitor the change in submersion height during the experimental and practical applications.

The absorption performance of the venturi reactor varied significantly due to the submersion height compared with the smooth variation in the venturi–bubbling reactor. As shown in Figure 4, the absorption efficiency increased substantially from 17.38% to 59.11% when the submersion height was increased from 100 to 700 mm. This was because the submersion height directly affected the amount of liquid released from the venturi reactor. Reducing submersion height also reduced the time for the toxic gas to penetrate the absorber bed and the adequate gas–liquid contact time at the same gas flow rate based on the observations.<sup>25,26</sup> It was reflected in a significant increase in gas concentration at the venturi reactor outlet and a decrease in mass transfer performance.

Figures 5 and 6 show the effect of absorber concentration and pH on the absorption of spilled  $\text{H}_2\text{S}$ , the reaction mechanism of which can be approximated by eqs 2, 3, and 4:

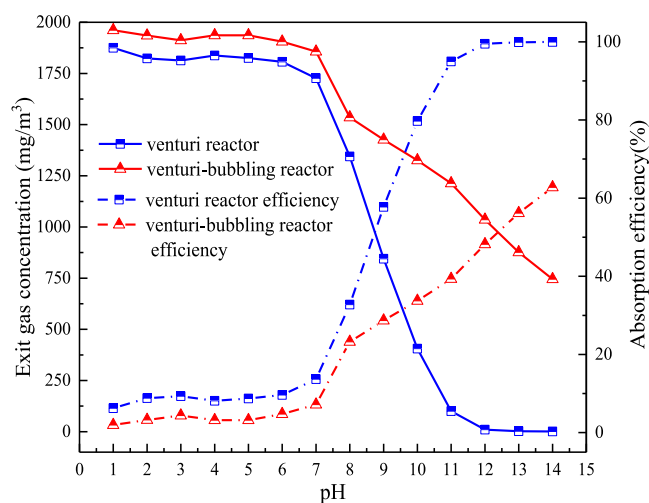
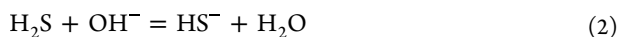
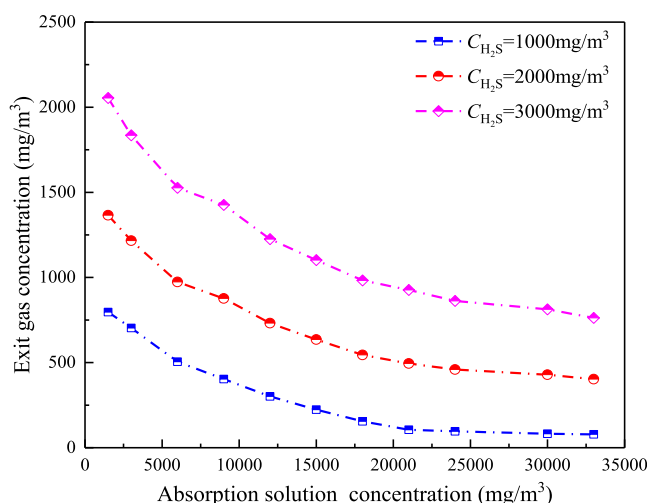
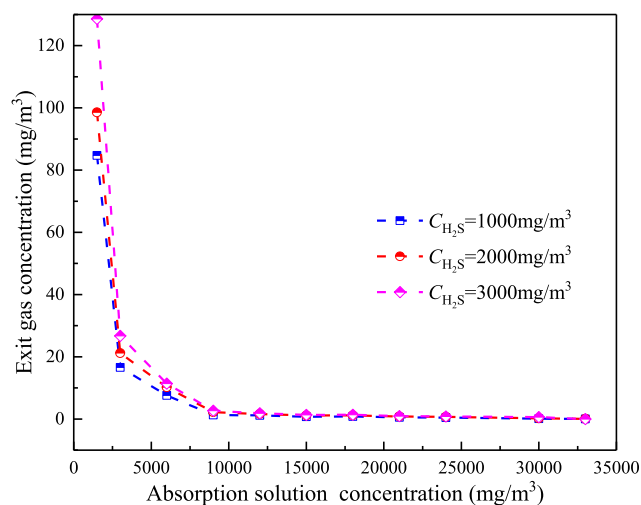


Figure 5. Effect of pH on the absorption performance rate.

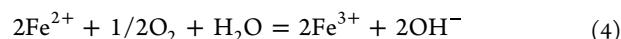
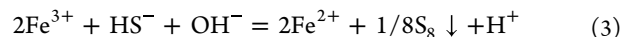


(a) Venturi reactor



(b) Venturi–bubbling reactor

Figure 6. Effect of absorbing solution concentration ( $\text{Fe}^{3+}$ ) on the absorption performance rate.



In the wet oxidation processes, the potassium hydroxide solution is usually used as the activating solution for absorption,  $\text{Fe}^{3+}/\text{Fe}^{2+}$  as the catalyst, and  $\text{O}_2$  as the oxidizing agent.<sup>20</sup> Although pH does not influence the overall reaction process, it significantly affects the capture and dissolution of  $\text{H}_2\text{S}$  gas. As shown in Figure 5, the absorbent solution hardly reacted with the  $\text{H}_2\text{S}$  gas at a solution pH below 7. Notably, the alkalinity of the absorbent solution played a decisive role in the first step of the reaction. When the pH increased to 7–10, the  $\text{H}_2\text{S}$  concentration at the outlets of the venturi and bubbling reactors decreased rapidly with increasing pH. That is, the absorption performance increased significantly. As the pH increased to 11–12, the decreasing trend of the  $\text{H}_2\text{S}$  concentration at the outlets of the venturi and bubbling reactors with increasing pH became slower. When the pH exceeded 13, the  $\text{H}_2\text{S}$  concentration at the outlets of the venturi and bubbling reactors remained unchanged. Then, the pH of the absorption solution increased, and the overall

absorption performance did not change. It indicated that the absorption of toxic gases must occur in an alkaline environment with an optimum pH of 13.

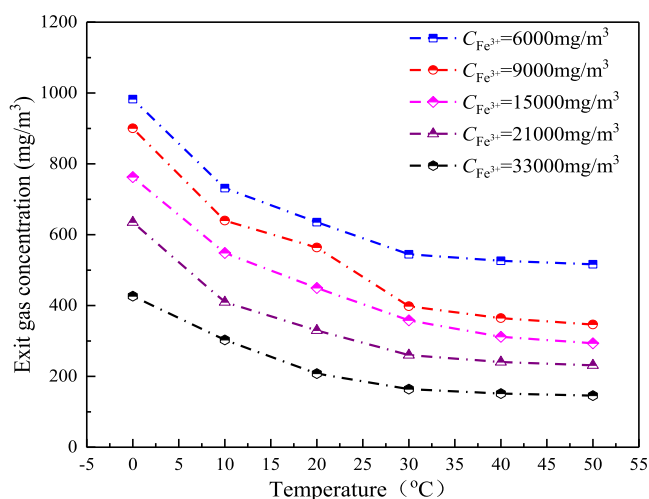
As shown in Figure 6, the  $\text{H}_2\text{S}$  concentration at the outlets of both the venturi reactor and the venturi–bubbling reactor first decreased with the increase in  $\text{Fe}^{3+}$  concentration and then remained constant; the absorption performance significantly improved for both.

At a  $\text{Fe}^{3+}$  concentration of  $9000 \text{ mg/m}^3$ , the venturi–bubbling reactor outlet concentration was always below the emergency emission standard at an inlet  $\text{H}_2\text{S}$  concentration of  $3000 \text{ mg/m}^3$ , indicating that the increase in absorbent concentration significantly enhanced the absorption performance of the toxic gas. It was also found that the absorption effect hardly changed in the venturi reactor once the  $\text{Fe}^{3+}$  concentration in the absorption solution increased to  $21000 \text{ mg/m}^3$ . For the venturi–bubbling reactor, when the  $\text{Fe}^{3+}$  concentration in the absorption solution increased to  $12000 \text{ mg/m}^3$ , the absorption effect hardly changed with the increase in  $\text{Fe}^{3+}$  concentration. The absorption performance did not show a continuous improvement with increasing  $\text{Fe}^{3+}$  in the absorption solution. Instead, there existed optimal parameters that yielded the best absorption performance. However, an increase in  $\text{Fe}^{3+}$  concentration increased the viscosity of the absorbent solution and the absorption pressure drop of the toxic gas. Therefore, the optimum  $\text{Fe}^{3+}$  concentration for the emergency disposal process for leaked  $\text{H}_2\text{S}$  was  $21000 \text{ mg/m}^3$ .

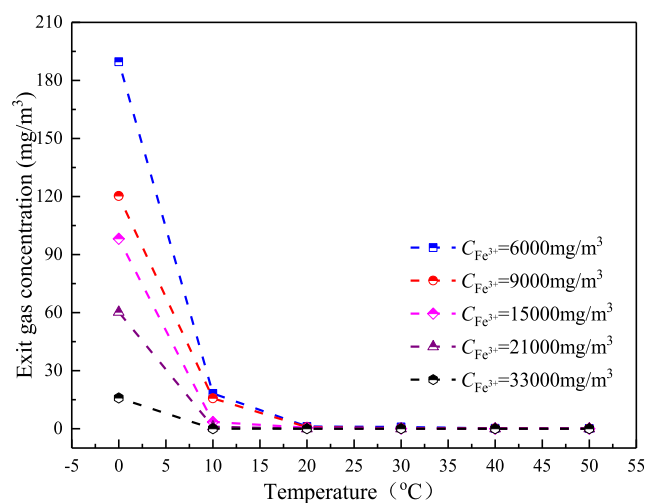
Figure 7 shows the effect of temperature on the  $\text{H}_2\text{S}$  absorption performance. As the decomposition temperature of the chelating agent in the catalyst was  $52 \text{ }^\circ\text{C}$ , the test range was chosen from  $0$  to  $50 \text{ }^\circ\text{C}$ . The absorption performance first remained constant and then decreased with the decrease in the temperature of the absorption solution. The absorption efficiency started to fall at  $10 \text{ }^\circ\text{C}$ – $15 \text{ }^\circ\text{C}$ , and the absorption efficiency dropped significantly at  $0 \text{ }^\circ\text{C}$ – $10 \text{ }^\circ\text{C}$ . When the ambient temperature approached  $0 \text{ }^\circ\text{C}$ , the absorbent solution could no longer deal effectively with leaked  $\text{H}_2\text{S}$ . Hence, the best working temperature range for  $\text{H}_2\text{S}$  emergency disposal equipment was  $15 \text{ }^\circ\text{C}$ – $50 \text{ }^\circ\text{C}$ , which could also be relaxed to  $10 \text{ }^\circ\text{C}$ – $50 \text{ }^\circ\text{C}$  as appropriate.

If the working ambient temperature is not within this range, then suitable insulation treatment, such as adding cooling equipment and insulation modules, must be included. When applied on a large scale, appropriate increases are required to reduce the concentration of the absorption solution according to the environment. In summer, when the temperature is higher, the concentration of absorption solution can be reduced to save maintenance costs. In winter, when the temperature is low, the concentration of the absorption solution can be increased appropriately during emergencies to improve the handling capacity of the installation.

As the experimental platform used a recyclable  $\text{Fe}^{3+}/\text{Fe}^{2+}$  process, the off-gas from the loading and unloading processes outside the sulfur-containing wastewater treatment plant was used as the gas source for the field performance tests in the experiments. When the gas flow rate was  $200 \text{ m}^3/\text{h}$ , the effect of operating time on the  $\text{H}_2\text{S}$  absorption effect was considered. The actual spill emergency disposal site equipment is generally used for less than 24 h. Therefore, the experiments tested the absorption performance of the equipment under continuous 48 h operation of the experimental platform. As shown in Figure 8, despite fluctuations in the inlet gas concentration ( $50$ – $3000 \text{ mg/m}^3$ ), the absorption efficiency of the toxic gas  $\text{H}_2\text{S}$  hardly



(a) Venturi reactor



(b) Venturi–bubbling reactor

Figure 7. Effect of temperature on the absorption performance rate.

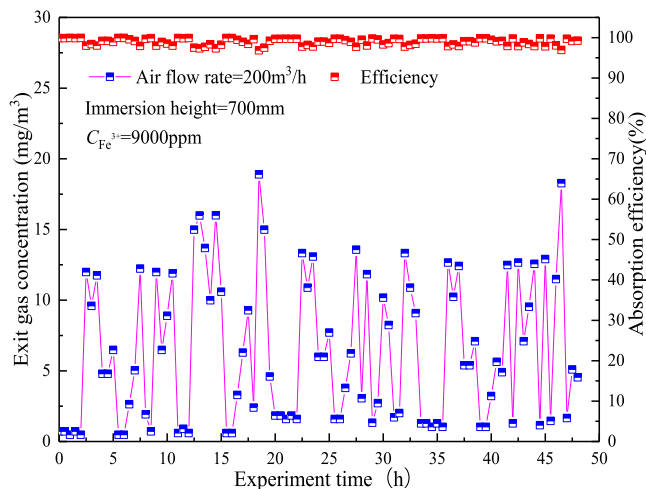


Figure 8. Effect of operating time on the absorption performance rate.

changed significantly during the test time, always being high at 90%. Also, the outlet concentrations were all below the emergency discharge standard. It showed that, on comparing



(a) Bubble reactor (1000Nm<sup>3</sup>/h)  
4000mm\*1900mm\*2600mm



(b) Venturi-bubbling reactor (500Nm<sup>3</sup>/h)  
1720mm\*1720mm\*2000mm

Figure 9. Physical diagram of coupling reactor and bubbling reactor.

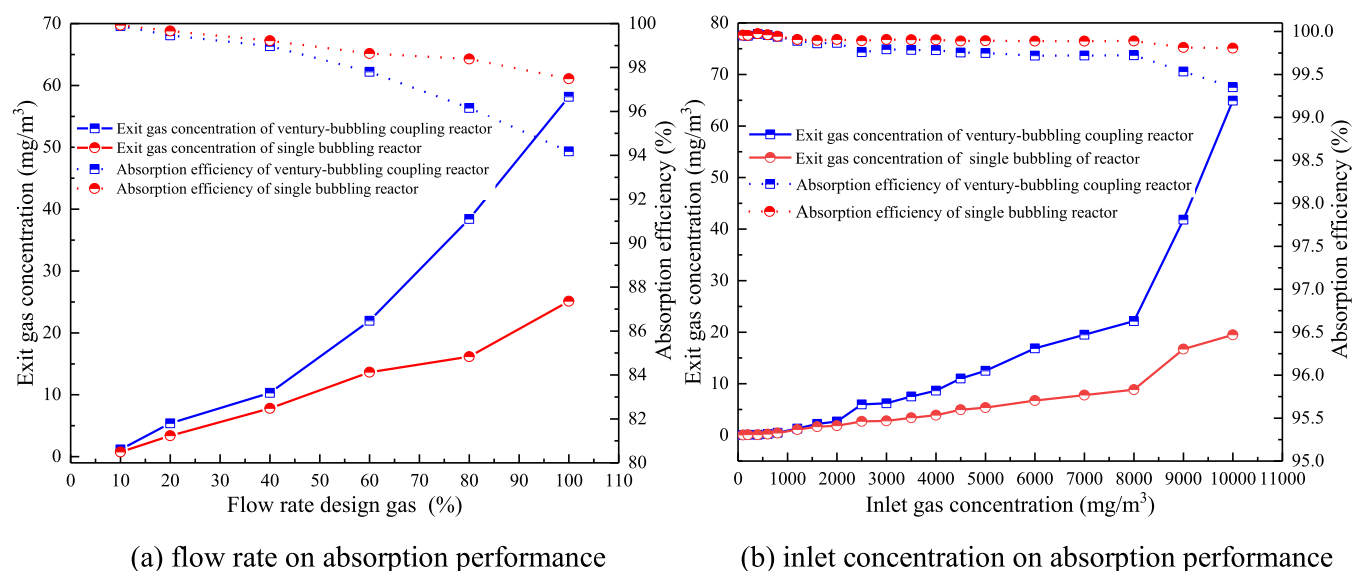


Figure 10. Absorption performance of different operating parameter.

the developed process and experimental platform with the bubbling reaction process alone, the equipment size was significantly reduced, had good absorption performance over a more extended duration, and fully met the emergency needs of the H<sub>2</sub>S leakage site.

Hence, on comparing the venturi and bubbling reactors, it was found that the venturi reactor was more sensitive to the changes in operating parameters. In contrast, the bubbling reactor had better redundancy and satisfied the contingency requirements under more fluctuations in operating parameters, but the equipment was extensive and huge. However, considering the simple structure of the venturi reactor and the lower pressure, it was ideally suited for pilot-scale, or even industrial plant, coarse treatment applications. The integration

and coupling of the venturi and bubbling reactors allowed for better absorption performance in a minimum size of equipment.

The absorption performance of the venturi-bubbling coupling reactor was compared with that of the previously designed bubbling reactor through experiments, and the evolution law of absorption by the coupling reactor was analyzed (as shown in Figure 9 and Figure 10).

Figure 9 depicts a physical diagram of both reactors, where the left picture represents the bubbling reactor (4000 × 1900 × 2600 mm<sup>3</sup>), and the right picture represents the venturi-bubbling coupling reactor (1720 × 1720 × 2000 mm<sup>3</sup>). That is to say, the volume of the coupled reactor accounts for 29.94% of that in the separate bubbling reactor. The absorption



capacity of both devices to leakage H<sub>2</sub>S was tested at 0–100% design gas and 0–10 000 ppm.

As seen from Figure 10, when the inlet concentration is at ERPG-2 emission standard level or below, maximum gas volume for coupled process is about 60% of design value while maximum inlet gas volume is about 90% for single bubbling reactor under same inlet concentration; thus making maximum applicable gas volume for coupled process two-thirds that of larger scale bubbling reactor.

Also, for the same gas volume and concentration range (0–10 000 mg/m<sup>3</sup>), both the bubbling reactor and coupling reactor are capable of processing the gas. In Figure 9(a), it can be observed that the outlet concentration of the bubbling reactor is lower than that of the coupling reactor shown in Figure 9(b). The maximum applicable concentration for the coupling reactor is 8000 ppm, whereas for the bubbling reactor it reaches approximately 10 000 ppm, accounting for an approximate difference of 80%, which meant the coupling process can achieve 80% of the performance exhibited by a separate bubble reactor, while occupying merely 29.94% of its volume.

Although the coupled process exhibits lower absorption performance compared to a single bubbling reactor, it offers advantages such as smaller equipment size, maximum gas volume (about 66.67% of the latter), and maximum applicable concentration (80.0% of the latter). Consequently, it achieves higher absorption efficiency with ample gas redundancy, making it more suitable for emergency systems.

#### 4. CONCLUSIONS

In this study, an experimental platform was designed for the absorption of leaked H<sub>2</sub>S by the venturi–bubbling reactor on a pilot scale. The effects of critical operating parameters, such as inlet gas flow rate, inlet H<sub>2</sub>S concentration, absorption solution submersion height, absorption solution concentration, and solution temperature, on the absorption performance of leaked H<sub>2</sub>S were tested. The main findings were as follows:

- (1) The concentration of outlet H<sub>2</sub>S gas increased with the concentration of inlet H<sub>2</sub>S gas and decreased significantly with the increase in gas flow rate. After the inlet concentration was higher than 2000 mg/m<sup>3</sup>, the absorption efficiency of the venturi reactor did not change and remained at around 50%, which was only suitable for the coarse treatment of toxic gases.
- (2) The absorption performance of the venturi–bubbling reactor for H<sub>2</sub>S gas decreased first with the increase in submersion height and then remained stable. After the inlet height approached 600 mm, the overall absorption efficiency of the venturi–bubbling reactor remained constant, with an absorption efficiency of more than 97%.
- (3) The best Fe<sup>3+</sup> concentration for leaked H<sub>2</sub>S absorption was 21 000 mg/m<sup>3</sup>. The absorption performance was stable at first and then decreased with the increase in the temperature of the absorbent solution, and the best working temperature range was 10 °C–50 °C.
- (4) Within the range of fluctuating inlet gas concentrations (50–3000 mg/m<sup>3</sup>), the pilot-scale experimental platform had an outlet concentration below the emergency emission standard for 48 h, which could fully satisfy the real emergency needs of the site.

- (5) The absorption reactor utilizing the venturi-bubbling coupling process achieves approximately 80% of the performance exhibited by the traditional single bubble process while utilizing only 29.94% of its volume.

#### AUTHOR INFORMATION

##### Corresponding Author

Yi Zheng – State Key Laboratory of Chemicals Safety, Qingdao 266071, P. R. China; SINOPEC Research Institute of Safety Engineering Company, Limited, Qingdao 266071, P. R. China; [orcid.org/0000-0002-8296-3040](https://orcid.org/0000-0002-8296-3040); Email: [Zhengy.qday@sinopec.com](mailto:Zhengy.qday@sinopec.com)

##### Authors

Guangwen Zhang – State Key Laboratory of Chemicals Safety, Qingdao 266071, P. R. China; SINOPEC Research Institute of Safety Engineering Company, Limited, Qingdao 266071, P. R. China

Yong Zhao Dong – SINOPEC Health, Safety and Environmental Protection Management Department, Beijing 100728, P. R. China

Complete contact information is available at:

<https://pubs.acs.org/10.1021/acsomega.4c01346>

##### Notes

The authors declare no competing financial interest.

#### ACKNOWLEDGMENTS

G.Z. and Y.Z. contribute equally to the article. The authors are grateful to the financial supports by the Natural Science Foundation of China (Grant No. 52106123).

#### REFERENCES

- (1) Kailasa, S. K.; Koduru, J. R.; Vikrant, K.; et al. Recent progress on solution and materials chemistry for the removal of hydrogen sulfide from various gas plants [J]. *J. Mol. Liq.* **2020**, *297*, 111886.
- (2) Georgiadis, A. G.; Charisiou, N. D.; Goula, M. A. Removal of hydrogen sulfide from various industrial gases: A review of the most promising adsorbing materials [J]. *Catalysts* **2020**, *10* (5), 521.
- (3) Ubando, A. T.; Del Rosario, A. J. R.; Chen, W. H.; et al. A state-of-the-art review of biowaste biorefinery [J]. *Environmental pollution* **2021**, *269*, 116149.
- (4) Chan, Y. H.; Lock, S. S. M.; Wong, M. K.; et al. A state-of-the-art review on capture and separation of hazardous hydrogen sulfide (H<sub>2</sub>S): Recent advances, challenges and outlook [J]. *Environ. Pollut.* **2022**, *314*, 120219.
- (5) Li, M.; Ren, L.; Gu, Z.; et al. Insight into the enhancement effect of amino functionalized carbon nanotubes on the H<sub>2</sub>S removal performance of nanofluid system [J]. *Journal of Hazardous Materials* **2023**, *458*, 131977.
- (6) Wang, J.; Yang, C.; Zhao, Y. R.; et al. Synthesis of porous cobalt oxide and Its performance for H<sub>2</sub>S removal at room temperature [J]. *Ind. Eng. Chem. Res.* **2017**, *56*, 12621–12629.
- (7) Zhao, Y.; Yang, C.; Zhang, H.; et al. Effect of surface hydrophilicity on the desulfurization performance of ZnO/SiO<sub>2</sub> composite [J]. *Journal of Inorganic and Organometallic Polymers and Materials* **2019**, *29* (4), 1192–1197.
- (8) Zhao, Y.; Zhang, Z.; Yang, C.; Fan, H.; Wang, J.; Tian, Z.; Zhang, H.; et al. Critical role of water on the surface of ZnO in H<sub>2</sub>S removal at room temperature [J]. *Ind. Eng. Chem. Res.* **2018**, *15366*–15374.
- (9) Gonzalez, K.; Boyer, L.; Almouchachar, D.; et al. CO<sub>2</sub> and H<sub>2</sub>S absorption in aqueous MDEA with ethylene glycol: Electrolyte NRTL, rate-based process model and pilot plant experimental validation [J]. *Chemical Engineering Journal* **2023**, *451*, 138948.

- (10) Park, J.; Lee, S. Y.; Kim, J.; et al. Energy, safety, and absorption efficiency evaluation of a pilot-scale H<sub>2</sub>S abatement process using MDEA solution in a coke-oven gas [J]. *Journal of Environmental Chemical Engineering* **2021**, *9* (1), 105037.
- (11) Üresin, E.; Sarac, H b; Sarioglan, A.; et al. An experimental study for H<sub>2</sub>S and CO<sub>2</sub> removal via caustic scrubbing system [J]. *Process Safety and Environmental Protection* **2015**, *94*, 196–202.
- (12) Kang, J. H.; Yoon, Y.; Song, J. Effects of pH on the simultaneous removal of hydrogen sulfide and ammonia in a combined absorption and electro-oxidation system [J]. *Journal of hazardous materials* **2020**, *382*, 121011.
- (13) Su, H.; Wang, S.; Niu, H.; et al. Mass transfer characteristics of H<sub>2</sub>S absorption from gaseous mixture into methyldiethanolamine solution in a T-junction microchannel [J]. *Separation & Purification Technology* **2010**, *72* (3), 326–334.
- (14) Yang, S.; Zhao, X.; Sun, W.; et al. Effect of ring baffle configuration in a self-priming venturi scrubber using CFD simulations [J]. *Particuology* **2019**, *47*, 63–69.
- (15) Azizi, M.; Biard, P.-F.; Couvert, A.; et al. Simulation of hydrogen sulphide absorption in alkaline solution using a packed column [J]. *Environmental Technology* **2014**, *35*, 3105–3115.
- (16) Jiao, W.; Yang, P.; Liu, G.; et al. Selective absorption of H<sub>2</sub>S with high CO<sub>2</sub> concentration in mixture in a rotating packed bed [J]. *Chemical Engineering and Processing* **2018**, *129*, 142–147.
- (17) Wang, Y.; Liu, Y.; Wang, Y. Oxidation absorption of hydrogen sulfide from gas stream using vacuum ultraviolet/H<sub>2</sub>O<sub>2</sub>/ urea wet scrubbing system [J]. *Process Safety and Environmental Protection* **2020**, *140*, 348–355.
- (18) Zou, C.; Zhao, P.; Ge, J.; Qin, Y.; Luo, P.; et al. Oxidation/adsorption desulfurization of natural gas by bridged cyclodextrins dimer encapsulating polyoxometalate [J]. *Fuel* **2013**, *104*, 635–640.
- (19) Schiavon Maia, D. C.; Niklevicz, R. R.; Arioli, R.; et al. Removal of H<sub>2</sub>S and CO<sub>2</sub> from biogas in bench scale and the pilot scale using a regenerable Fe-EDTA solution [J]. *Renewable Energy* **2017**, *109*, 188–194.
- (20) Safarzadeh-Amiri, A.; Walton, J.; Mahmoud, I.; et al. Iron(III)-polyphosphates as catalysts for liquid redox sulfur recovery process [J]. *Applied Catalysis B Environmental* **2017**, *207*, 424–428.
- (21) Schiavon Maia, D. C.; Niklevicz, R. R.; Arioli, R.; Frare, L. M.; Arroyo, P. A.; Gimenes, M. L.; Pereira, N. C.; et al. Removal of H<sub>2</sub>S and CO<sub>2</sub> from biogas in bench scale and the pilot scale using a regenerable Fe-EDTA solution [J]. *Renewable Energy* **2017**, *109*, 188–194.
- (22) Jiang, X.; Wu, J.; Jin, Z.; Yang, S.; Shen, L.; et al. Enhancing the removal of H<sub>2</sub>S from biogas through refluxing of outlet gas in biological bubble-column [J]. *Bioresour. Technol.* **2020**, *299*, 122621.
- (23) Zhan, J.; Wang, B.; Zhang, L.; et al. Simultaneous absorption of H<sub>2</sub>S and CO<sub>2</sub> into MDEA+PZ aqueous solution in a rotating packed bed [J]. *Ind. Eng. Chem. Res.* **2020**, *59* (17), 8295–8303.
- (24) Rattanaya, T.; Manmeen, A.; Kongjan, P.; et al. Upgrading biogas to biomethane using untreated groundwater-NaOH absorbent: Pilot-scale experiment and scale-up estimation for a palm oil mill [J]. *Journal of Water Process Engineering* **2021**, *44*, 102405.
- (25) Breitenmoser, D.; Papadopoulos, P.; Lind, T.; et al. Droplet size distribution in a full-scale rectangular self-priming Venturi scrubber with liquid film injection [J]. *International Journal of Multiphase Flow* **2021**, *142*, 103694.
- (26) Zhou, Y.; Sun, Z.; Gu, H.; et al. Structure design on improving injection performance for venturi scrubber working in self-priming mode [J]. *Progress in Nuclear Energy* **2015**, *80*, 7–16.